

Low-temperature photoemission study of the surface electronic structure of Si(111) 7×7

R. I. G. Uhrberg*

Department of Physics and Measurement Technology, Linköping University, S-581 83 Linköping, Sweden

T. Kaurila

Department of Applied Physics, University of Turku, 20014 Turku, Finland

Y.-C. Chao

Department of Physics and Measurement Technology, Linköping University, S-581 83 Linköping, Sweden

(Received 26 March 1998)

The electronic structure of the Si(111) 7×7 surface has been studied in detail at a sample temperature of 55 K with high-energy-resolution angle-resolved photoemission. The photoemission spectra show a previously undetected surface-state structure at ≈ 0.5 eV below the Fermi level that we assign to dangling-bond states located mainly to the adatoms near the corner holes of the 7×7 reconstruction. Detailed dispersion curves obtained at 55 K are presented for the three uppermost, dangling-bond derived, surface states. Surface sensitive Si $2p$ spectra obtained in this low-temperature study still show a comparatively broad line shape. Possible reasons for this are discussed. [S0163-1829(98)51128-9]

Angle-resolved photoemission studies have consistently reported the existence of three surface-state bands on the Si(111) 7×7 surface. The two bands closest to the Fermi level (E_F) are interpreted as dangling-bond derived and the third surface state is associated with back-bonds. By combining photoemission results with information obtained from scanning tunneling microscopy (STM) a rather detailed assignment of the surface states has evolved in terms of adatom, rest atom, and back-bond states. There are basically three types of dangling bonds on the 7×7 surface. In a unit cell there are 6 rest atom dangling-bond electrons, 1 corner-hole dangling-bond electron, and 12 dangling-bond electrons associated with the adatoms. The two uppermost surface-state bands observed by photoemission (commonly denoted S_1 and S_2) show only a weak dispersion indicating a rather localized nature in real space.¹ This has been verified in STM studies in which an assignment of S_1 and S_2 were made.^{2,3} The S_1 state, at ≈ -0.15 eV (relative to E_F), is located on the adatoms and S_2 , at ≈ -0.9 eV, is located to the rest atom positions and at the corner-hole atoms. Since both the rest atom and corner-hole dangling-bond derived states are well below E_F they must be doubly occupied. This situation can be obtained by a transfer of dangling-bond electrons from the adatom states that are higher in energy compared to the rest atom and corner-hole states. This leads to a situation where the 12 adatom dangling-bond electrons are reduced to 5 electrons.⁴ In a band picture these five dangling-bond electrons can give rise to two fully occupied bands and one half full surface band in the 7×7 surface Brillouin zone (SBZ). Photoemission shows significant emission at E_F implying that the 7×7 surface is metallic which is consistent with the odd number of adatom dangling-bond electrons. The five adatom electrons reveal themselves as the rather broad S_1 state in photoemission.

In this Rapid Communication we have reexamined the surface states of the 7×7 surface in an angle-resolved photoemission study employing high-energy resolution at a low

temperature (55 K). The spectra exhibit a new surface-state structure S'_1 located at ≈ -0.5 eV, which can be followed in the inner half of the 1×1 SBZ. The low-temperature spectra also provide more detailed information on the structure closest to E_F . At approximately half the distance between $\bar{\Gamma}$ and \bar{M} of the 1×1 SBZ there is a sharp minimum in the dispersion. The shape of the dispersion curve very much resembles what is observed for the Si(111) $\sqrt{3}\times\sqrt{3}$:Sn surface that is metallic with a half-full dangling-bond band.⁵ A detailed dispersion of the S_2 surface band is also obtained in this low-temperature study. The dispersion of S_2 is similar to what has been reported earlier.¹

The photoemission study was performed at beam line 33 at the Maxlab synchrotron radiation facility in Lund, Sweden. A spherical grating monochromator produces usable light in the range 14–200 eV. The electrons are analyzed by a hemispherical analyzer (VG, ARUPS 10) equipped with an electronic lens that can be run at different angular resolutions. The valence-band spectra were obtained with a photon energy of 21.2 eV with a total energy resolution of <50 meV (analyzer and monochromator) and an angular resolution of $\pm 2^\circ$. Surface sensitive Si $2p$ core-level spectra were also recorded in this study at total energy resolutions between 70 and 90 meV. The n -type (Sb, $3\ \Omega\ \text{cm}$) Si(111) sample was chemically etched before it was inserted into the vacuum system.⁶ After extensive outgassing the silicon oxide was removed by direct current heating to $\approx 930^\circ\text{C}$. After the initial cleaning the sample was flashed to $\approx 1150^\circ\text{C}$ several times. This procedure produced valence-band spectra with well-developed surface-state structures and high-quality Si $2p$ spectra. Low-energy electron diffraction (LEED) showed a sharp 7×7 pattern at room temperature. At 55 K the 7×7 LEED spots were sharper and the background intensity was lower than at room temperature, as expected. No other diffraction features than the 7×7 spots could be observed in the LEED pattern. Neither the valence-band spectra nor the

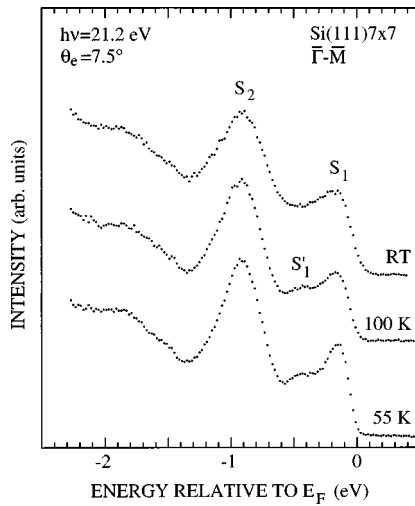


FIG. 1. Angle-resolved valence-band spectra obtained from the Si(111)7 \times 7 surface at three different sample temperatures. The new surface state S'_1 appears in the low-temperature spectra at ≈ 0.5 eV below E_F .

Si 2*p* core-level spectra showed any indication of contamination at 55 K. Thus, the spectra presented here are representative of clean low-temperature Si(111)7 \times 7 surfaces.

Figure 1 shows a set of valence-band spectra obtained for different sample temperatures at an emission angle of 7.5° along the $\bar{\Gamma}$ - \bar{M} direction. In the room temperature spectrum the two surface-state structures S_1 and S_2 appear at ≈ -0.15 and ≈ -0.9 eV, respectively. Even though S_1 and S_2 are well separated in energy (0.75 eV) there is a significant emission between these states that gives rise to an asymmetric shape of the S_1 structure. The origin of the asymmetry is revealed in the low-temperature spectra. A third surface-state structure, S'_1 , which has not been reported previously, can be identified at an energy position of ≈ -0.5 eV. S'_1 is clearly observable in spectra obtained at 100 K and it becomes even more well defined at 55 K as the S_1 structure also becomes narrower.

We have mapped the dispersion of the surface states S_1 , S'_1 , and S_2 along the $\bar{\Gamma}$ - \bar{M} and $\bar{\Gamma}$ - \bar{K} lines of the 1 \times 1 SBZ. Spectra measured at 55 K were used to get the most detailed information about the dispersions. Figure 2 shows spectra for various emission angles in the $\bar{\Gamma}$ - \bar{M} direction. The S'_1 structure is resolved from the S_1 peak up to an emission angle of 10°. Due to the increase in the S_1 intensity and a downward shift of that peak it is hard to resolve the S'_1 structure in the spectra between 12.5° and 17.5°. For larger emission angles S'_1 can be identified in the spectra but the intensity is too small to obtain a reliable dispersion. In addition to the S'_1 structure, we also get new information about S_1 from these spectra. Earlier room temperature studies have reported a characteristic intensity increase of the $\bar{\Gamma}$ structure at approximately half the distance between $\bar{\Gamma}$ and \bar{M} as is also observed here. What we additionally find is that the intensity increase is accompanied by a dispersion resulting in a rather sharp energy minimum.

The dispersions of the S_1 , S'_1 , and S_2 surface states are plotted in Fig. 3 along both the $\bar{\Gamma}$ - \bar{M} and $\bar{\Gamma}$ - \bar{K} directions. The S'_1 state seems to have a small upward dispersion in the $\bar{\Gamma}$ - \bar{M}

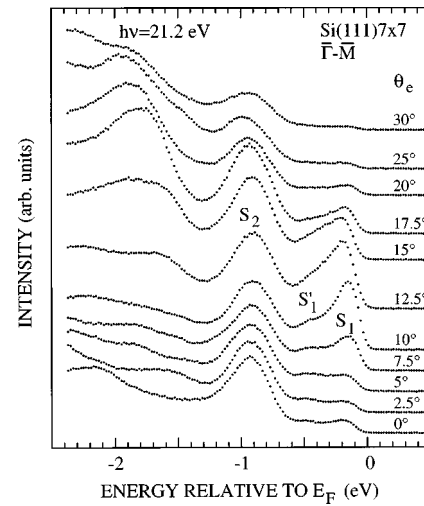


FIG. 2. Valence-band spectra obtained at 55 K for various emission angles along the $\bar{\Gamma}$ - \bar{M} direction of the 1 \times 1 SBZ.

direction while it does not exhibit any discernible dispersion in the $\bar{\Gamma}$ - \bar{K} direction. The S_2 structure shows strong emission intensity all the way to the 1 \times 1 SBZ boundary. S_2 exhibits the largest dispersion in the $\bar{\Gamma}$ - \bar{K} direction with the highest energy position at $k_{\parallel} \approx 0.44 \text{ \AA}^{-1}$. In the $\bar{\Gamma}$ - \bar{M} direction we note a slight upward dispersion to be followed by a downward dispersion closer to \bar{M} . The total bandwidth of S_2 from the data in Fig. 3 is 0.12 ± 0.03 eV. The dispersion features and the bandwidth of the S_2 surface state is similar to what was reported in an earlier room temperature study.¹ The dispersions of the S_1 and S_2 surface states are normally plotted in the 1 \times 1 SBZ but the extreme points of the dispersions do not seem to be related to the 1 \times 1 symmetry. It is intriguing to note that the most pronounced features of the dispersion coincide with the symmetry points of the 7 \times 7

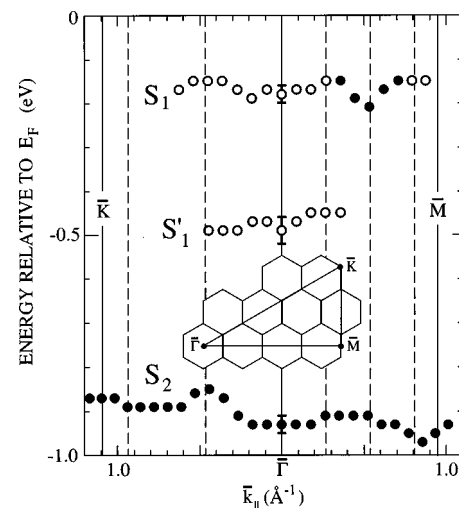


FIG. 3. Dispersion of the S_1 , S'_1 , and S_2 surface states along the $\bar{\Gamma}$ - \bar{K} and $\bar{\Gamma}$ - \bar{M} symmetry lines of the 1 \times 1 SBZ. The inset shows the symmetry points of the 1 \times 1 SBZ and several 7 \times 7 SBZ's. The dashed lines indicate the positions of $\bar{\Gamma}_{7\times 7}$ points along the \bar{k}_{\parallel} axis. Filled circles indicate strong emission intensity. The error bars at the $\bar{\Gamma}$ point indicate the maximum uncertainty in the energy positions.

SBZ, i.e., the minimum of S_1 at 0.54 \AA^{-1} along $\bar{\Gamma}-\bar{M}$ and the maximum of S_2 at 0.44 \AA^{-1} along $\bar{\Gamma}-\bar{K}$; both occur at $\bar{\Gamma}$ points of the 7×7 SBZ in a repeated zone scheme (see the inset in Fig. 3). The maximum at the $\bar{\Gamma}_{7 \times 7}$ point in the $\bar{\Gamma}-\bar{K}$ direction does not show up at the $\bar{\Gamma}_{7 \times 7}$ points probed in the $\bar{\Gamma}-\bar{M}$ direction. Thus for the results to be consistent with the 7×7 periodicity, the S_2 structure has at least to consist of two components. It has not been possible to directly resolve any additional structure in the S_2 peak but the strong asymmetry of the S_2 peak in the 25° spectrum in Fig. 2 provides indirect evidence for more than one contribution. The observed dispersion of S_2 is a result of both rest atom and corner-hole dangling-bond contributions to the S_2 emission. The S_2 emission should correspond to the 12 electrons of the rest atom states and it should most likely also include the 2 electrons associated with the corner-hole states. Thus in a band-structure picture, S_2 is the result of seven bands that are close in energy.

Based on a band-structure picture and the five adatom dangling-bond electrons the photoemission results for S_1 and S'_1 can be interpreted in terms of two rather flat doubly occupied bands (open circles at ≈ -0.5 and -0.15 eV, respectively) and one half full dispersive band (solid circles near $\bar{\Gamma}_{7 \times 7}$).

An alternative way to discuss the photoemission data would be to use a more localized picture since the separation between atoms on the 7×7 surface is quite large. STM studies have shown that electrons with initial energies corresponding to the S_2 state are located to the rest atoms and to the atoms in the corner holes. Electronic states with energies corresponding to S_1 were found to be associated with the adatoms in the 7×7 unit cell. All 12 adatoms are not equivalent according to the STM study.^{2,3} Due to the stacking fault in one half of the unit cell there is a charge transfer between the halves that breaks the symmetry. Besides this difference between the faulted and unfaulted halves, the six adatoms within one half of the unit cell also appear inequivalent. In the filled state STM images the adatoms next to a corner hole appear higher than the adatoms on the sides of the adatom triangles. Thus in a localized ‘‘atomiclike’’ picture we could expect at least two different binding energies for the adatom dangling bonds in each half of the unit cell, which leads in principle to a total of four possible energies for the adatom dangling bonds. This difference suggests that it is possible to associate the photoemission structures S_1 and S'_1 with different adatoms in the 7×7 unit cell.

From theoretical calculations of the electronic structure⁷⁻¹² we can derive a plausible assignment of the S'_1 structure. A common result of the calculations is that they find the adatom states close to the Fermi level. In the calculations by Qian and Chadi⁷ and Fujita, Nagayoshi, and Yoshimori,⁸ the rest atom states and the corner-hole state are found to be close in energy while Brommer and co-workers^{11,12} find a strong corner-hole state within 0.2 eV from the Fermi level. Only the results by Qian and Chadi⁷ and Fujita, Nagayoshi, and Yoshimori,⁸ are consistent with STM observations and we therefore exclude the corner-hole state as a possible explanation for the S'_1 peak. In the study by Fujita, Nagayoshi, and Yoshimori⁸ the band structure was

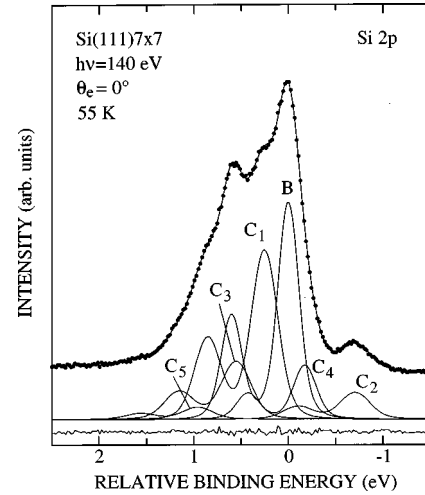


FIG. 4. Surface sensitive Si $2p$ core-level spectrum from the Si(111) 7×7 surface obtained at 55 K. A curve fitting analysis of the spectrum results in a decomposition into one bulk and five surface components. The energy shifts of the components C_1 , C_2 , C_3 , C_4 , and C_5 are 253, -706 , 553, -188 , and 961 meV, respectively.

presented for a few \bar{k}_{\parallel} points in the 7×7 SBZ along with spatially resolved contour maps of the charge density for selected electron energies. For the adatom manifold, which crosses the Fermi level, the lowest states were found to preferentially locate charge on the adatoms next to the corner hole. These are the atoms that appear brightest in STM images of the adatoms when tunneling out of occupied states. The electronic states on adatoms next to a corner hole were also found to be lowest in energy in the calculation by Stauffer and co-workers^{9,10} where density of state curves were presented. Based on the STM results and on the available theoretical results, we assign the S'_1 band to adatom dangling bonds mainly located to the adatoms next to the corner holes.

Si $2p$ core-level spectra were also recorded from the 7×7 surface at 55 K as a complementary way of verifying a high surface quality. Another incentive to carry out core-level studies of the 7×7 surface was the very high spectral resolution obtained on the Si(001) $c(4 \times 2)$ surface under the same experimental conditions.¹³ Figure 4 shows a normal emission Si $2p$ spectrum obtained from the same 7×7 surface as that from which the valence-band data were recorded. Surprisingly, this spectrum is very similar to those obtained at 120 K in an earlier study.¹⁴ The significant improvement in resolution observed for the Si(001) $c(4 \times 2)$ surface is not observed for the 7×7 surface. Increased energy resolution and decreased phonon broadening by measuring at lower temperatures do not reveal any further details in the complicated surface sensitive Si $2p$ spectrum of the 7×7 surface. It seems that an intrinsic limit is reached in the resolution for the Si $2p$ core level of the 7×7 surface. The reason for the comparatively broad Si $2p$ spectra from the 7×7 surface is most likely to be found in the detailed atomic and electronic structure of the 7×7 surface. From STM studies it is known that there is a charge asymmetry between the faulted and unfaulted halves of the 7×7 unit cell. Furthermore, there is an inequivalence between adatoms within each half of the

7×7 cell as discussed above. Thus the structural features such as adatoms, rest atoms, second layer atoms, etc., do not represent homogeneous sets of atoms. Within each group one can expect slightly different Si $2p$ binding energies due to details in the charge transfer that would manifest itself as a broadening of the Si $2p$ components. The inequivalence between the two halves would also affect the width of the ‘‘bulk’’ component since the escape depth is only ≈ 3 Å at a photon energy of 140 eV.¹⁴ The lack of improvement in resolution in the Si $2p$ spectra from the 7×7 surface unfortunately hampers any dramatic progress in the understanding/assignment of the surface core-level shifts.

Three recent high-resolution Si $2p$ studies^{14–16} agreed on the main conclusions that the rest atoms give rise to the component C_2 shifted to lower binding energies and that the adatom component C_3 is shifted toward higher binding energies compared to the bulk component. In the study by LeLay *et al.*¹⁵ a singlet component was introduced in the fit at a binding energy of -0.41 eV relative to the bulk component. It was assigned to a crystal-field splitting of the rest atom component. This component was not present in the decompositions of the Si $2p$ core-level spectra presented by Karlsson *et al.*¹⁴ or by Paggel *et al.*¹⁶ In Fig. 4 we show a fit to the 55 K spectrum¹⁷ that is in very good agreement with that of Ref. 14. We do not find any need for an extra singlet component contrary to the study by LeLay *et al.*¹⁵ Based on our present results and two of the earlier studies^{14,16} we find that there is no reason to introduce crystal-field splitting of the rest atom state as an explanation of the Si $2p$ line shape.

In this paper we have reported a surface state S'_1 on the Si(111) 7×7 that becomes separated from the S_1 surface state at low temperatures. From comparisons with earlier STM studies, as well as theoretical studies of the surface states of the 7×7 surface, we assign S'_1 to dangling-bond states mainly located at the adatoms near the corner holes of the 7×7 reconstruction. Detailed dispersion curves for the dangling-bond derived surface states S_1 , S'_1 , and S_2 have been presented based on the 55 K photoemission data. The dispersion curves show features that can be attributed to the 7×7 SBZ, such as the minimum of the S_1 band at a $\bar{\Gamma}_{7\times 7}$ point. Since the dispersions do not fully follow the 7×7 periodicity the assignment of the dispersion features to the 7×7 SBZ must be regarded as tentative at this stage. The surface sensitive Si $2p$ core-level spectrum recorded at 55 K showed no improvement in terms of resolution, contrary to what has been observed for the Si(001) $c(4\times 2)$ surface. The intrinsically large widths of the bulk and surface components of the Si $2p$ spectrum were attributed to the inherent inequivalence between the surface atoms in the faulted and unfaulted halves of the 7×7 unit cell. In accordance with two earlier high-resolution core-level studies of the 7×7 surface^{14,16} we do not find any evidence for crystal-field splitting of the rest atom component as was recently suggested.¹⁵

Support from the Maxlab staff is gratefully acknowledged. This work was supported by the Swedish Natural Science Research Council.

*Author to whom correspondence should be addressed. FAX: (+46) 13 13 75 68. Electronic address: rub@ifm.liu.se

¹P. Mårtensson, W.-X. Ni, G. V. Hansson, J. M. Nicholls, and B. Reihl, Phys. Rev. B **36**, 5974 (1987), and references therein.

²R. J. Hamers, R. M. Tromp, and J. E. Demuth, Phys. Rev. Lett. **56**, 1972 (1986).

³R. J. Hamers, R. M. Tromp, and J. E. Demuth, Surf. Sci. **181**, 346 (1987).

⁴J. E. Northrup, Phys. Rev. Lett. **57**, 154 (1986).

⁵T. Kinoshita, S. Kono, and T. Sagawa, Phys. Rev. B **34**, 3011 (1986).

⁶A. Ishizaka and Y. Shiraki, J. Electrochem. Soc. **133**, 666 (1986).

⁷G.-X. Qian and D. J. Chadi, Phys. Rev. B **35**, 1288 (1987).

⁸M. Fujita, H. Nagayoshi, and A. Yoshimori, Surf. Sci. **242**, 229 (1991).

⁹L. Stauffer, P. Sonnet, and C. Minot, Surf. Sci. **371**, 63 (1997).

¹⁰L. Stauffer, S. Van, D. Bolmont, and J. J. Koulmann, Solid State Commun. **85**, 935 (1993).

¹¹K. D. Brommer, B. E. Larson, M. Needels, and J. D. Joannopoulos, Jpn. J. Appl. Phys., Part 1 **32**, 1360 (1993).

¹²K. D. Brommer, M. Galván, A. Dal Pino, Jr., and J. D. Joannopoulos, Surf. Sci. **314**, 57 (1994).

¹³R. I. G. Uhrberg, T. Kaurila, and Y.-C. Chao, Maxlab Activity Report No. 1996, p. 130 (unpublished).

¹⁴C. J. Karlsson, E. Landemark, Y.-C. Chao, and R. I. G. Uhrberg, Phys. Rev. B **50**, 5767 (1994).

¹⁵G. LeLay, M. Göthelid, T. M. Grekh, M. Björkquist, U. O. Karlsson, and V. Yu. Aristov, Phys. Rev. B **50**, 14 277 (1994).

¹⁶J. J. Paggel, W. Theis, K. Horn, Ch. Jung, C. Hellwig, and H. Petersen, Phys. Rev. B **50**, 18 686 (1994).

¹⁷The spin-orbit split between the $p_{1/2}$ and $p_{3/2}$ was 602 meV and the branching ratio was 0.48. A Lorentzian width of 80 meV was used for all components. The Gaussian width of the bulk component was 220 meV, and for the surface components C_1 , C_2 , C_3 , C_4 , and C_5 the Gaussian widths were 290, 330, 330, 240, and 330 meV, respectively.